

<https://doi.org/10.1038/s44264-024-00014-4>

Power-law productivity of highly biodiverse agroecosystems supports land recovery and climate resilience

Check for updates

Masatoshi Funabashi^{1,2} ✉

Transformative change in primary food production is urgently needed in the face of climate change and biodiversity loss. Although there are a growing number of studies aimed at global policymaking, actual implementations require on-site analyses of social feasibility anchored by ecological rationale. This article reports the in-depth characterizations of low-input mixed polyculture of highly diverse crops managed on the self-organization of ecosystems, which performed better compared to conventional monoculture methods in Japan and Burkina Faso. Analyses on crop productivity and diversity showed that the primary production of ecosystems followed a power law, and through the underlying mechanisms excelled in (1) promoting diversity and total quantity of products along with the rapid increase of in-field biodiversity, especially useful for the recovery of local regime shift in a semi-arid environment; (2) a fundamental reduction of inputs and environmental load; and (3) ecosystem-based autonomous adaptation of the crop portfolio to climatic variability. The overall benefits imply substantial possibilities of a new typology of sustainable farming for smallholders sensitive to climate change, which could overcome the historical trade-off between productivity and biodiversity based on the human-guided augmentation of ecosystems.

Many studies have sounded alerts about global ecological deterioration due to the accelerating impacts of human activity in the last century (e.g., refs. 1–4). The 6th mass extinction is considered underway in a wide range of biotic communities, including primary forests⁵, vertebrates⁶, and insect fauna⁷.

These impacts are largely due to the primary food production on land and have caused critical environmental shifts in marine ecosystems⁸. Here, the agricultural sector is responsible for 25% of greenhouse gases (GHGs)⁹, and it has disrupted global biochemical flows and biosphere integrity¹⁰. However, interactive responses to changes in human activities, material cycles, and biodiversity distribution, including effects induced by climate change mitigation and conservation activities, are extremely complex and difficult to simulate. Globally assessed scenarios (e.g., refs. 4,11) are not capable of predicting actual social emergencies, such as the COVID-19 pandemic, and cannot promptly address the root causes. Moreover, the importance of an integrated approach to the science of climate and biodiversity changes and the development of coherent policies has only recently been realized (e.g., ref. 12). Current economic theory and practice do not sufficiently incorporate a valuation of biodiversity and multiple ecosystem

services¹³; we need to take comprehensive measures interconnecting direct drivers of ecosystem deterioration and underlying economic, social, and technological causes, in order to regenerate the ecologically driven material cycles and substantially reducing agricultural inputs and runoff^{3,14}.

Future scenarios toward sustainable land use aimed at recovery of biodiversity and the carbon cycle have been suggested with various forms of global-scale simulations (e.g., refs. 15,16). On the other hand, despite their scale, these studies are based on databases that do not necessarily encompass the practical social-ecological contexts required for an actual implementation. The interactions of many parameters and the complexity of community dynamics have largely been ignored (e.g., in a food-system change scenario¹⁵, the cross-field phosphorus cycle¹⁷ and management breakthrough on the carbon cycle¹⁸ are not included; in a global afforestation scenario¹⁶, the implausibility of afforestation of naturally maintained grasslands and savannas and thermodynamic trade-off between tree cover increase and consequent diminishment of albedo¹⁹ are not considered). The ground truth is often ignored even in basic statistical studies; this makes the applicability of global scenarios to actual situations quite elusive—while 84% of some 570 million farms are owned by smallholders producing on less

¹Sony Computer Science Laboratories, Inc., Tokyo, Japan. ²Research Division on Social Common Capital and the Future, Kyoto University Institute for the Future of Human Society, Kyoto, Japan. ✉e-mail: masa_funabashi@csl.sony.co.jp

than 2 ha, estimates of the total surface of smallholds vary from 12% to 40% of the global farmland depending on the method of measurement²⁰. Although implications from global studies of course-grained models may still be meaningful to orient policy direction, concrete evaluation and management criteria for individual farms need to be developed from operational case studies in connection with a realistic driving force.

Through recent meta-analysis, significant research gaps are identified as practical problems²¹ in (P1) how to double the incomes and productivity of small-scale food producers; (P2) how to make food production more environmentally sound and more resilient to climate shocks and other disasters; and (P3) how to respond the needs of smallholders and their families within local contexts with the support of original data.

In order to convert the majority of food producers, especially resource-, knowledge-, and technology-deprived smallholders into positive drivers of biodiversity, on-site tailoring and proactive management of agrobiodiversity in a comprehensive social-ecological context are important leverage points^{3,22}. An essential pillar of transformative change in food production is to deliver a management-intensive typology of sustainable practices that contains interfaces with the diversity and uniqueness of real-world operations on a scientific basis, which has been studied in the field of open complex systems science^{14,23,24}. We need complementarity between a general theory based on averaged statistics and deep analyses of significant individual cases in order to make progress toward the inclusion of neglected diversity. With the rise of big data, such a paradigm has emerged in the management of living systems, such as in precision medicine (e.g., N-of-1 studies²⁵ and other longitudinal deep phenotyping), yet to be applied for Planetary Health, which is a solution-oriented interdisciplinary field and social movement on the well-being of all living organisms through analyzing and addressing the impacts of human disruption to the Earth's natural systems²⁶. This study aims to provide the agroecological rationale for such a novel paradigm through elaborate characterizations of pioneering cases that are compatible in production modality and scale with the application to the grass-root majority of world food production.

Crop production at ecological optimum

Empirical studies in ecology have revealed the positive contribution of species diversity and the symbiotic relationship between plants to the primary production of ecosystems at the community level (e.g., ref. 27), especially in relation with surface patterns that follow power-law distribution^{28,29}. Although knowledge of self-organized natural vegetation constitutes a better understanding of community dynamics and has been used for planning conservation practices, little of it has been applied to crop production.

In order to bridge these gaps between agronomy and ecology, synecological farming (synecoculture) was conceived based on the synecology, i.e., the study of communities of organisms and their interactions within an ecosystem and with the environment, later called community ecology³⁰. It

takes advantage of the sustainable productivity of self-organized vegetation that occurs when there is an extremely high diversity of crops^{14,31}. The principle of production in synecoculture is fundamentally different from those of other low-input organic and natural farming methods that are limited in their association and rotation of a few crops (e.g., ref. 32). In contrast to the conventional definition of productivity based on a single crop and a field environment controlled toward its physiological optimum, synecoculture relies on the primary production of a mixed community that comprises tens to hundreds of edible plant species; this sort of production is known as augmentation of the ecological optimum (explained in Box 1).

Specific research questions based on the synecoculture farming system are formulated as follows, which aim to address P1–P3 from synecological perspectives:

(Q1) How do community dynamics, in terms of biodiversity and productivity, self-organize and respond to climatic variability, separately from the effects of social confounding factors such as market access and farmers' literacy?

(Q2) Especially, what is the dynamical property of productivity beyond simply aggregated means? Is there any relation between productivity fluctuation and resilient property?

(Q3) Concerning these characteristics, is there a possibility to yield a common principle beyond the particularities of species composition, soil conditions and climatic differences?

Results

Symbiosis-dominant ecosystems with crops

To evaluate the self-organization process of a mixed community of crops, a practice on a 420-sq.m plot in the temperate zone (Oiso, Japan) was chosen to measure the species-wise surface at the early stage of synecoculture introduction (Fig. 2 a1–a4: field A, see Methods). The inverse cumulative distribution of the species diversity on the surface was closer to a power-law distribution than an exponential distribution, implying that the symbiotic interactions between plants are inherent besides the competition for resources (Fig. 3a).

The probability density of the species-wise surface in each 2-sq.m measurement section also followed a power law (Fig 10 (top) of Supplementary Information). The relative degree of symbiotic relationship can be compared with the parameter λ and showed that naturally occurring spontaneous species (usually considered to be weeds) form vegetation patterns that contain more positive interactions (λ closer to zero) than the introduced crop species. This tendency was also observed in another classification of edible and non-edible plants based on past usage in synecoculture practices. Positive diversity responses to climate variability were also dominant in spontaneous species (see Fig. 7 of Supplementary Information). The direct implication is that the coexistence of naturally occurring non-edible species serves as a substantial source of symbiotic gain for the whole community dynamics that promotes ecological succession, and it

Box 1. | Integrated model of physiological and ecological optima (IMPEO)³⁰

The physiological optimum is the basis of monoculture optimization in agronomy, which is generally expressed as a unimodal distribution along the environmental gradient (Fig. 1a). In actual ecological situations, however, isolated growth is not fully attained and mixed communities are prevalent, which results in diverse shifting, division, and modification of the growth curve leading to the emergence of ecological niches (Fig. 1b). Random harvesting from various environments asymptotically converges the mean productivity to a normal distribution under the mean environmental conditions of the samples (Fig. 1c). According to the nature of competition with other species, the plants can qualitatively be classified as those with central or marginal competence (orange and blue distributions, respectively, in Fig. 1). Such differences generally produce

competitive loss and symbiotic gain of productivity, and both contribute to the total overyielding in mixed communities (green distribution in Fig. 1c).

The contribution of symbiotic gain to the total overyielding in mixed polyculture could become increasingly significant as the mean environment shifts from a physiologically favorable condition (yellow background) to the marginal ranges (orange background), and create new stretches of arable land in harsh conditions where little monoculture growth can be expected (red background).

See the Supplementary Information Fig. 6 for the multi-dimensional version of IMPEO.

may contribute to the productivity of crops and other edible plants through an overall increase in resources such as soil organic matter and soil microbial activity³³.

Production experiments

The productivity of synecoculture in temperate and semi-arid tropical zones was tested in two farms, on a 1000 sq.m farm in Ise, Japan over the course of four years (Fig. 2 b1, b2: field (B) and on a 500 sq.m farm in Mahadaga, Burkina Faso over the course of three years (Fig. 2 c1–c5: field (C)). The probability density of product-sales data based on asynchronous thinning of highly diverse mixed polyculture showed a long-tail distribution that largely deviated from a conventional normal distribution (Fig. 4 a, b and Fig. 5 a, b), and it followed power law (See Fig. 10 (middle and bottom) of Supplementary Information, and examples of harvests in Fig. 2 b2 of the main text), regardless of the differences in climate region and species composition.

Despite the no-input practice except water and introduction of seeds and seedlings, on-site observation implied overall and multiple increases in ecosystem functions along with the ecological succession in the fields, such as improvement in crop yield, the establishment of a complex food chain that supported ecological regulation of pests, thick development of porous soil structure, increased humus and soil organic matter, improved water retention and permeability, and the resulting activation of soil microbiota (see e.g., Fig. 2 c4, c5, Fig 11 a1 and b1 of Supplementary Information, and refs. 24,30,34).

The average profitability (measured as gross sales minus costs) of synecoculture in the field B rose 2.35- to 3.87-fold, which corresponds to an estimated 0.981- to 1.16-fold increase in harvest biomass, compared with the conventional databases of all scales and small scale (<0.5 ha) (see the description of the relative biomass ratio BR in Methods). Compared with the median (and 25th and 75th percentiles) of conventional market gardening, the profitability of synecoculture in the field C rose 88.0(202/54.4)-fold, which corresponds to an estimated 33.8(49.6/25.1)-fold increase in harvest biomass, on average over two 18-month periods before and after November 2016 under different social conditions. In particular 121(278/74.9)-fold increase in profitability corresponding to an estimated 37.8(55.3/28.0)-fold increase in harvest biomass under high market accessibility, and a 55.0(126/34.0)-fold increase in profitability corresponding to a 29.9(43.8/22.2)-fold increase in harvest biomass under low market accessibility (see Methods). The on-site comparison at the field C showed that synecoculture excelled in showing 258-fold increase profitability in correspondence with an estimated 12.4-fold harvest biomass compared with the five other simultaneously tested alternative methods of sustainable farming.

A most dramatic change was the local reversal of the regime shift in the field C. From an analysis of satellite images taken before the experiment, the vegetation patches that surrounded the field C corresponded to spotted vegetation patterns that strongly implied warning signals of imminent desertification³⁵. The subsequent intensive introduction of 150 edible plant species, including 40 staples, reestablished a lush ecosystem that maintained high productivity year-round that had positive regeneration effects on neighboring plots (Fig. 2 c1–c3). The established ecosystem comprised typical plant types that reached a mature vegetation succession stage, such as pioneering annual and perennial plants, shrubs and vines, light-demanding trees and shade-tolerant trees.

Climate resilience

In all of the experiments conducted in the fields A, B and C, a significant positive correlation of plant species diversity with the fluctuation components of major meteorological parameters was observed, which could not be totally reduced to a correlation with the mean components (Figs. 3b, 4c, and 5c of the main text and Figs. 7–9 of Supplementary Information). The observed biodiversity response can be considered as an adaptive diversification of the species composition to climatic variability³¹ rather than seasonal patterns in community dynamics, because seasonality was weaker in the fluctuation than in the mean components due to the non-linear relationships between the mean and standard deviation of meteorological

parameters (bottom line of Figs. 7–9 of Supplementary Information). A possible origin of the positive correlation between the meteorological variance and plant species diversity could be found in evolutionary acquired biodiversity maintenance mechanisms, because increasing diversity to cope with environmental fluctuation generally contributes to sustain ecological community. Such community-level responses might constitute a fundamental mechanism to augment the climate resilience by mainstreaming biodiversity in food production³⁶, which could provide an enhanced portfolio of agrobiodiversity beyond substitution and relocation of major crops³⁷, and thereby enlarge the range of options to cope with the inescapable global biodiversity redistribution under climate change³⁸ and keep the food systems within the planetary limits^{15,39}.

Discussion

One of the greatest challenges in this study that seems contradictory to conventional monoculture methods is the stabilization of yield that relies on ecological niche formation. The rationale of synecoculture lies in productivity at the community level with an extensive portfolio of products and reduced input costs, which is compatible with the primary production of self-organized plant communities in natural environment³⁰. In Fig. 10 of Supplementary Information, although the fitted Pareto distributions for all experiments are situated in the parameter range where analytical mean converges to a finite value (i.e., $a > 1$), a large deviation is inherent even at the annual scale (the 12-month gross sales ranged between 56 and 141% of the total average for the field C and was between 27 and 214% of the total average for the field B). Therefore, productivity in terms of arithmetic means is not a stable indicator for management. Still, the cumulative cost-benefit ratio converged to a higher level of performance compared with the conventional and other alternative methods (Fig. 11 a2 and b2 of Supplementary Information), which conforms to the theoretical prediction of power-law productivity and stability of harmonic means in our previous study³¹. This is due to the positive correlation of productivity with introduced species diversity that develops over time, which is particularly enhanced in the ecological optimum production and performs increasingly better in marginal environments for both gains in gross sales and cost reductions (see total overyielding in Fig. 1 of the main text and Fig. 6 of Supplementary Information for the theoretical predictions, and Fig. 11 a1 and b1 of Supplementary Information for the measured data).

Not only the higher productivity of the field C, but also the ecological optimization with synecoculture could rebuild the power-law distribution of patch patterns and may help to prevent state shifts in the farm plots near the living area in a semi-arid environment^{35,40}. The recovery and enhancement of diverse vegetation in farm plot represents a major shift from negative to positive externality on biodiversity in crop production¹⁴, which is also compatible with massive greening initiatives to reestablish a viable environment against desertification (e.g., ref. 41). It also sets a new baseline of increased crop diversity and yield against the declining trend in dryland¹¹, which can minimize land clearing and protect habitats of threatened large mammals especially in sub-Saharan Africa⁴², where animal-source foods are nutritionally valuable in food-deficient settings⁴³. Given the importance of sustainability of smallhold farms and the positive social-ecological impacts that synecoculture could have, international initiatives in ECOWAS are being formed to better utilize the capacity of ecological optimum production, with a short-term goal to provide healthy and balanced diets to 3.5 million people impacted by COVID-19⁴⁴.

An important yet unconventional methodological challenge in this study is the adoption of an in-depth profiling strategy of selected significant cases, rather than a cohort study, in order to properly respond to the research questions Q1–Q3 based on ecological theories. The discoveries in this study have not been able to be addressed in other global ecological models and large-scale cohort studies, particularly in terms of the temporal resolution of data and high level of crop diversity, and it leads to the formation of the following methodological recommendations R1–R3 as the responses to Q1–Q3, respectively, which are applicable to other practices aiming at ecological optimization:

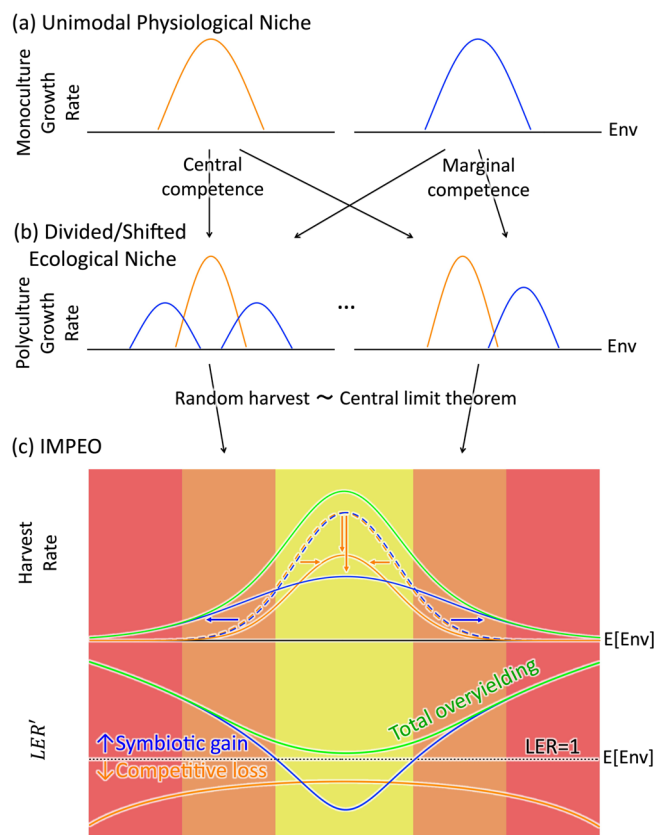


Fig. 1 | Relationship between physiological and ecological optima and the total effect of overyielding. **a** *y*-axis: examples of physiologically optimum isolated growth rate versus *x*-axis: environmental parameters such as temperature, precipitation, sunlight, etc. **b** *y*-axis: primary productivity of various ecological niches in the same environment (*x*-axis) but mixed communities. **c** Top: random sampling from various niches in **a** (blue and orange dashed lines) and **b** (blue and orange solid lines) converges to normal distributions via the central limit theorem, their frequencies correspond to mean productivity measures such as harvest rate (*y*-axis) under averaged environmental conditions (*x*-axis). The overall productivity (green line) includes the productivities of plants of both growth-rate types. **c** Bottom: Effects of symbiotic gain (blue line and arrows) and competitive loss (orange line and arrows) of plants with marginal and central competence, respectively, measured as the land equivalent ratio (LER) on the scale of $LER' := \log(\log(LER) + 1)$. The main components of the total overyielding (green line) transit from centrally to marginally competent species as the environment shifts from the physiological optimum (yellow background) to marginal (orange background) and monoculture intolerant ranges (red background).

(R1) Low-input and high-biodiversity mixed association of crops supports the generation of symbiotic gain through the power-law distribution of edible biomass.

(R2) Characterization of power-law productivity should be conducted by the level of crop diversity, median and quartiles of total productivity, and cost-benefit ratio, which are more stable and practical indicators than the conventional arithmetic mean. The temporal fluctuation of productivity should be interpreted as the process of adaptive diversification of crop portfolio against environmental variability, which is the manifestation of an essential mechanism for sustaining biodiversity.

(R3) Despite the differences in crop portfolio, climate and soil conditions, the positive biodiversity response of the crops to climatic variability is the common feature we could expect as the general support of productivity, which is also a working hypothesis to be further verified in wider situations.

Based on R1–R3, supportive solutions S1–S3 can be proposed, which take other social contexts, technological and institutional leverages into account, and address the practical problems P1–P3:

(S1) Secure market access and increase literacy for the sales and utilization of a wider variety of potentially introducible crops. Big data science contributes to clarifying the dynamic reconfiguration of biodiversity in the face of climate change³⁸ and the future potential of ecological optimum production by estimating ecological niches of plant genetic resources (PGR) on a global scale³⁷.

(S2) Expand and improve access to PGR to realize a wider range of crop portfolios for ecological optimum production, and take advantage of increasing climatic variability and other environmental transitions. International seed banks towards the global adaptive diversification of PGR need to be developed, and benefit-sharing mechanisms from extensive use of PGR should be established in a way that is compatible with international legislation such as the Nagoya protocol³¹.

(S3) Provide education and training programs that teach the scientific principles of ecological optimum production, along with the analysis of various successful scenarios, and provide feedback and promotional material with actual data such as a certification of practices and produce. Providing access to the growing market of certified agricultural products with environmental concerns is a way to extend the distribution beyond the local demand. Data-driven marketing platforms and social networks have the potential to fill the gap between supply and demand in highly diverse crop portfolios and drastically reduce food waste.

Asia and sub-Saharan Africa will see the largest growth of agricultural emissions and will account for two-thirds of the increase in overall food demand by 2050⁴⁵. In the face of climate change and current pandemics, food systems that support these regions and other nations harboring smallholders need to be scaled bottom up and should realize synergy between provisioning and regulating services (including pathogen suppression) that have been historically put in massive trade-off in agricultural land use^{1,3}. In accordance with the biodiversity maintenance mechanisms that have been progressively revealed in the field of community ecology, our in-depth operational case studies imply that there exist fundamental principles that bring about such synergy through the leveraging of self-organized edible plant communities. Together with more comprehensive cohort studies in the future, it should lead to a novel typology for transformative change from resource- to management-intensive farming capable of creating essential biodiversity and ecosystem services in highly resilient form without resorting to fertilizers and agrochemicals. The diversity-driven productivity reported in this study has the potential to greatly improve improper agricultural practices, especially in the semi-arid environment, which coincides with an essential part of necessary conditions to upwardly recover the biodiversity decline in many global scenarios. With appropriate development of supportive information technologies^{24,46} and sustainable distribution networks for various farm products⁴⁷ and neglected and underutilized plant genetic resources⁴⁸, ecological optimum production could be applicable to small-scale farms less than 5 ha that make up 94% of agricultural holdings⁴⁹ and if combined with middle-scale farms less than 50 ha, produce up to 77% of the major commodities and nutrients in the world⁵⁰. Taken as a whole, the expansion and site-specific tailoring of human-augmented farming ecosystems has the potential to uplift the baseline of multiple ecosystem services and provide fundamental measures to cope with growing food demand and for proactive adaptation of various crop portfolio to climate change. It may in the long run introduce a human-driven form of resilience in biosphere integrity along with the expansion of essential human activities, by involving increasing population as a positive driver of biodiversity in Anthropocene^{14,30}.

Methods

Methods summary

We developed a theory that connects the differing definitions of productivity of monoculture-based optimization in agronomy and mixed community-based growth in ecology, which defines the protocol of synecological farming (synecoculture) as an extreme typology of plant food production based on self-organized ecological niches of a highly diverse community of crops mixed with other spontaneous vegetation.

Out of 60+ implementations, three small-scale plots representative of the good practice for smallholders were chosen in Japan and Burkina Faso, which were prepared following the protocol of synecoculture, and maintained without the use of tillage, fertilizers, or agrochemicals.

The species-wise surface was measured for a year in a harvest-free plot in Japan (field A) and was analyzed whether the vegetation patch pattern followed a power law that reflects symbiotic interaction between plants, or an exponential distribution based merely on the competition for resources.

Additionally, two production farms in Japan (field B) and Burkina Faso (field C) were chosen based on the completeness of three or more years of data on its productivity and cost. A wide variety of species-wise product sales was recorded and the statistical properties of the time series were analyzed in comparison with official statistics on productivity and the cost of conventional market gardening and other parallelly tested farming methods.

In all experiments, we compared the mean and variance parameters of meteorological records of the finest satellite open data with the observed plant diversity and analyzed statistical correlation that represented the biodiversity response to a changing environment during the growth period.

Simulation of the integrated model of physiological and ecological optima (IMPEO): Box 1 and Fig. 1

Based on ref.³⁰, we simulated a typical scenario of overyielding with a mixed polyculture of two plant species. First, let us describe the unimodal distribution of physiological growth of two species with the same physiological optimum range (Fig. 1a). We define this distribution as $U(Env; \nu_p)$ with an environmental parameter Env and its physiologically optimum value ν_p giving the maximum growth rate. The emerging ecological niches through interactions between the two species and the environment have several typologies, such as shifting and division, and other modifications of the growth curve, which are impossible to simulate precisely (Fig. 1b). Nevertheless, we will assume that there are qualitatively two different types of niche differentiation dynamics: (1) One plant type shows the superiority in growth of the physiological optimum to the other species (i.e., central competence expressed as the orange distributions in Fig. 1b); (2) The other plant type shows superiority in regard to growth in the marginal condition relative to the physiologically favorable range (i.e., marginal competence expressed as the blue distributions in Fig. 1b).

Let us describe the diverse ecological niches as $GR_c = EN_c(Env; \nu_c, \sigma_c)$ for centrally competent species and $GR_m = EN_m(Env; \nu_m, \sigma_m)$ for marginally competent species under the following assumptions, $\nu_c = \nu_m = \nu_p$ and $\sigma_c < \sigma_m$, where GR_c and GR_m stand for the growth rates, Env is an environmental parameter, and ν_c, ν_m and σ_c, σ_m are the means and standard deviations of Env for centrally and marginally competent species, respectively. For simplicity, we set the same surface ratio between centrally and marginally competent species, but the model is valid for any arbitrary ratio of mixed polyculture.

Random harvesting from all environments in those niches (i.e., random sampling from the growth rate distributions GR_c and GR_m) results in a normal distribution of mean productivity through the central limit theorem, such that $HR_c \sim N(E[Env]; \nu_c, \sigma_c)$ and $HR_m \sim N(E[Env]; \nu_m, \sigma_m)$, where $N(\cdot; \nu, \sigma)$ is a normal distribution with mean ν and standard deviation σ , HR_c and HR_m respectively represent the harvest rate of centrally and marginally competent species of the mean environmental parameter $E[Env]$ over the sampling. We can also obtain the mean monoculture productivity $U' \sim N(E[Env]; \nu_p, \sigma_p)$ by using the same sampling method, which results in $\sigma_c < \sigma_p < \sigma_m$. In Fig. 1c top, HR_c is depicted as an orange line, HR_m as a blue line, and $HR_c + HR_m$ as a green line. The parameters $\sigma_p = 20$, $\sigma_c = 19.7$, and $\sigma_m = 40$ were typical values chosen to illustrate the effects of competitive loss (orange arrows) and symbiotic gain (blue arrows in Fig. 1c bottom, the land equivalent ratio (LER)⁵¹ is the value calculated between the

mean monoculture productivity U' and its polyculture counterparts HR_c and HR_m , as $LER = \frac{HR_c + HR_m}{U'}$ (green line), and its species-wise components $\frac{HR_c}{U'}$ (orange line) and $\frac{HR_m}{U'}$ (blue line). These LER components are depicted on a scale of $LER' := \log(\log(LER) + 1)$, where the straight dotted black line is the separatrix $LER' = 0$ between symbiotic gain (upper part, $LER' > 0$) and competitive loss (lower part, $LER' < 0$).

Implementation of synecological farming (synecoculture) in Oiso and Ise, Japan and Mahadaga, Burkina Faso (Fig. 2)

Among more than 60 social implementation sites supported by scientific research of Sony CSL and UniTwin UNESCO CS-DC program during 2010–2023 (more than 50 in the Sahel⁴⁴ and 10 in Japan³⁴), we screened three representative cases that satisfied the following conditions:

1. One experimental field of the initial succession stage in Japan with a surface cover record of each vegetation without harvest (Field A).
2. One production site in Japan, which had sufficient diversity of crops and market access, and complete sales and cost records for three or more years (Field B).
3. One production site in the Sahel, which had sufficient diversity of crops and market access, and complete sales and cost records for three or more years (Field C).

These three sites established the highly biodiverse ecosystems following the protocol of synecoculture farming method, started from bare ground^{24,52,53}:

- Field A: From January 2010 to December 2011, randomly mixed communities of 52 edible plant species and other naturally occurring species on 420 sq.m without harvesting or watering and little weed maintenance in Oiso, Japan (GPS coordinates in decimal degrees: 35.31675, 139.32515). The plot was previously used for family gardening, but the vegetation was totally removed and the soil was homogeneously flattened by heavy machinery before the experiment.
- Field B: From April 2008, a preliminary observation of ecological niches of various plant species; from June 2010 to May 2014, a strategically mixed association of 133 edible plant species and other naturally occurring species on a commercial farm of 1,000 sq.m with harvesting and occasional watering and weed maintenance in Ise, Japan (GPS coordinates in decimal degrees: 34.53022, 136.6873). The plot was previously used as a conventional paddy field and was surrounded by other ones during the experiment.
- Field C: After the introduction of seeds and seedlings on March 2015, from June 2015 to May 2018, a strategically mixed association of 150 edible plant species on a commercial farm of 500 sq.m with harvesting, watering, and a small amount of weed maintenance in Mahadaga, Tapoa province, Burkina Faso (GPS coordinates in decimal degrees: 11.72328, 1.76136). The surrounding area including the plot was previously used for traditional market gardening, which became impossible due to soil degradation and was abandoned as bare land where natural regeneration did not occur.

For all implementations, only seeds and seedlings and necessary water as specified were introduced in the fields. No synthetic and organic fertilizers, no agrochemicals or other phytosanitary products, no ground cover materials, and no other amendments were used. No agricultural machinery was used, except for a small handy mower in the field B. No external financial support was given to the commercial synecoculture farms (field B and C).

Surface distribution analysis and correlation analysis between species diversity and meteorological parameters at the synecoculture field A (Fig. 3)

The covering surface of each plant species at low ground level in field A was measured with 2-step visual analog scale method (an extension of the traditional Brown-Blanquet method into percentile resolution to assess the

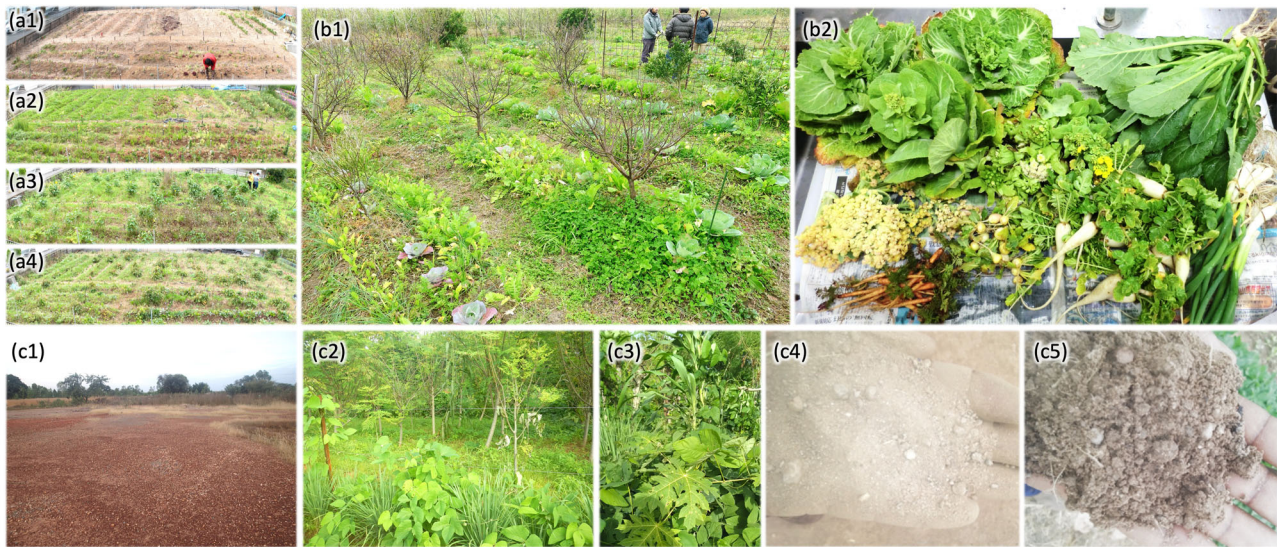


Fig. 2 | Studied synecoculture fields A (a1–a4), B (b1–b2), and C (c1–c5). a1–a4 Initial vegetation stages during the second year of crop species introduction from bare land in the temperate zone, in Oiso, Japan. After the construction of furrows in January 2010, pictures show the transition of vegetation during the second year in a1 early February, a2 early May, a3 late August, and a4 late October in 2011. b1 Pilot farm production experiment in the temperate zone, in Ise, Japan. Typical mixed polyculture state that augments diversity and productivity of vegetables in November is shown, with b2 an example of the products packed in a delivery box.

c1–c5 Reversal of the regime shift in the semi-arid tropics, in Mahadaga, Burkina Faso. c1 The control plot with no intervention remained bare for three years, while c2 the introduction of 150 edible species established vigorous ecosystems including c3 a strategic combination of crops with high density and vertical diversity. Partial regeneration of grass is observed in the background of c1, which appears to be a positive effect from the neighboring synecoculture field c2, c3. c4 Little organic matter is visible in the image of the topsoil of the control plot, which is in contrast to c5 showing the elaborated porous structure in the synecoculture plot.

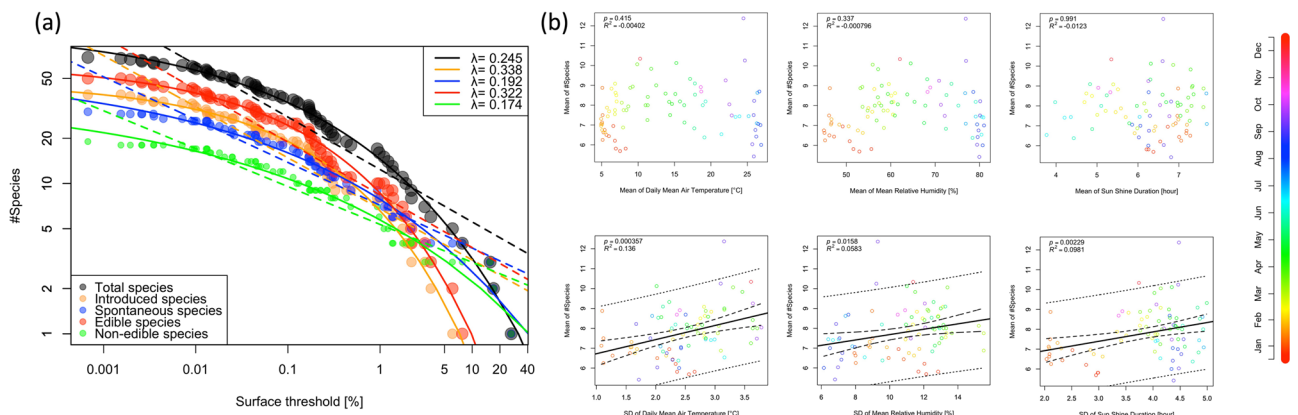


Fig. 3 | Spatial distribution and positive correlation with environmental variances in the initial stage of ecologically optimum crop growth in the temperate zone (field A). The initial-stage experiment in Oiso, Japan (Fig. 2 a1–a4) shows that a the estimated inverse cumulative distribution of the number of different plant species versus the percentage of the surface they occupy is closer to a power-law distribution that reflects symbiotic interactions $\lambda = 0$ than to an exponential distribution that merely reflects competition for resources $\lambda = 1$. b There exist positive correlations between the mean number of observed species and the variance of

meteorological parameters over the 30 days preceding the daily plot observation. There is no observable correlation with the means of the meteorological parameters. Mean plant species diversity versus mean and variance of three meteorological parameters are plotted with circles following the color gradient depicting the date. Black solid line: linear regression with less than 5% significance; dashed line: linear regression with 95% confidence; dotted line: linear regression with prediction intervals.

field vegetation cover³⁴ on 80 sections measuring 2 sq.m each, 22 times at an interval of 1 week to 1.5 months (about once every 2.3 weeks on average) at a frequency depending on the degree of growth during January – December 2011 (Supplementary Data 1). The observed plant species were categorized into (1) introduced crop species and (2) naturally occurring spontaneous species, which were also parallelly labeled as (3) edible species that were utilized and (4) non-edible species that were not yet utilized as synecoculture products.

In Fig. 3a, the inverse cumulative distribution of the number of different species is plotted with respect to the minimum threshold of yearly

averaged covering surface ratio. Theoretical models show that the size distribution of self-organized vegetation surface tends to an exponential distribution that reflects competition between plants for resources, but that it tends to a power-law distribution when there is locally symbiotic relationship^{28,29}. This assumption applies to the analysis of both the inverse-cumulative and non-cumulative distributions, since power-law and exponential functions are conserved under the transformation from a probability density to its cumulative distribution. The experiment in the field A focused on measuring the relative degree of contribution between local symbiotic interactions and resource competition at the inter-species level

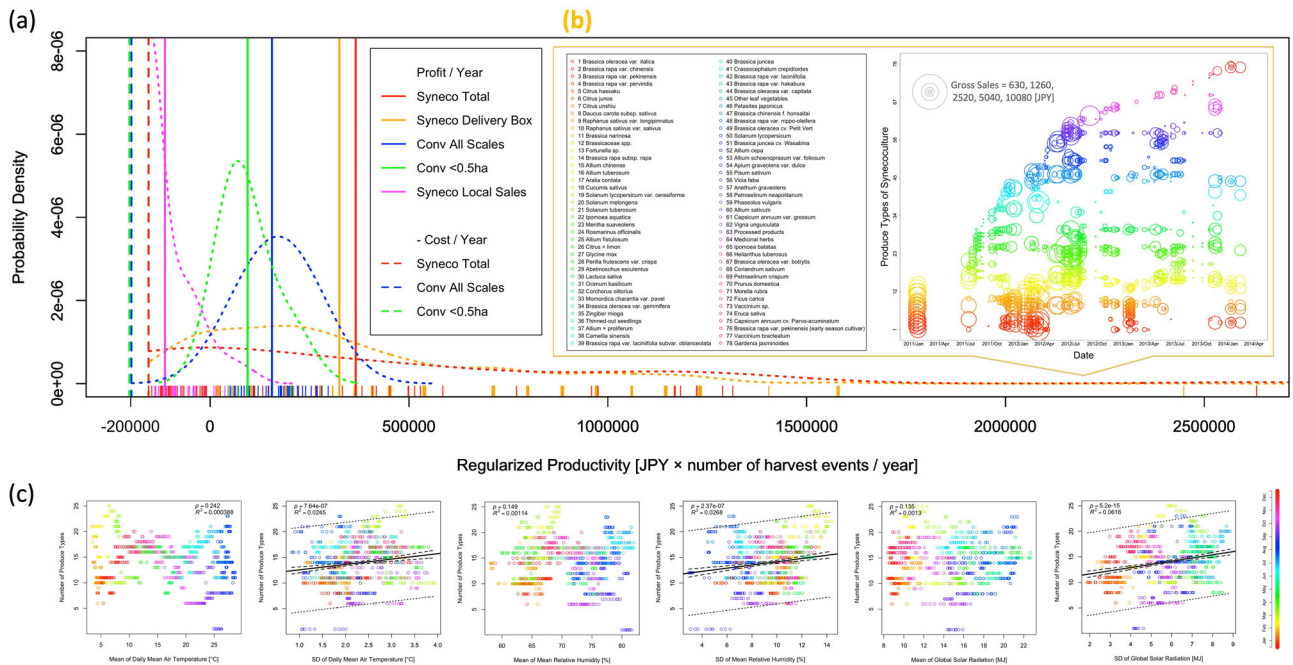


Fig. 4 | Productivity of synecoculture experiment in the temperate zone (field B). The four-year production experiment in Ise, Japan shows **a** a power-law distribution of product sales with **(b** in the orange rectangle) asynchronous harvests of 78 kinds of crop. The *x*-axis of **a** represents sales of each product in synecoculture on 1000 sq.m (regularized productivity is daily and species-wise productivity in terms of Japanese yen (JPY) multiplied by the number of harvest events per year for synecoculture or yearly reported profit for conventional methods), both with an offset of total costs in order to compare the yearly mean profits (vertical solid lines) and costs (vertical dashed lines) summed as positive and negative values, respectively (see Methods). The dotted lines on the *y*-axis represent the estimated probability distributions for each production category based on the data shown as the rug plots along the *x*-axis. In **b** left, the 78 academic names of total synecoculture products are shown as a list

with a color gradient, and the associated numbers define the value of the *y*-axis in **b** right, in which the sales for each product according to date on the *x*-axis is represented as the diameter of the circle with the same color gradient as the list. The correlational analysis in **c** shows significant positive correlations between the number of produce types from synecoculture and meteorological variances for each 30-day interval. There was no significant correlation with the mean of the meteorological parameters. Harvested crop diversity versus mean or variance of three meteorological parameters is plotted as circles following the color gradient of the date. Black solid line: linear regression with less than 5% significance; dashed line: linear regression with 95% confidence; dotted line: linear regression with prediction intervals.

(i.e., symbiotic gain and competitive loss in IMPEO) through an analysis of the species-wise averaged surface distribution. We devised an integrative model to evaluate the goodness of fit between the power-law and exponential distributions:

$$\log Y = A \cdot \text{BoxCox}(X, \lambda) + B$$

where $\text{BoxCox}(X, \lambda) = \begin{cases} \frac{X^\lambda - 1}{\lambda} & (1 \geq \lambda > 0) \\ \log X & (\lambda = 0) \end{cases}$ is the Box-Cox transformation with a continuous parameter $1 \geq \lambda \geq 0$, which converges to an exponential distribution $\log Y = A \cdot X - A + B$ in the $\lambda = 1$ case and a power-law distribution $\log Y = A \cdot \log X + B$ in the $\lambda = 0$ case. The fitting was performed using the `bcPower()` and `nls()` functions in R⁵⁴.

In Fig. 3b, mean species diversity in daily observed sections versus the mean and standard deviation of major meteorological parameters during the past 30 days from the observation (substantial growth period of the crops in the field) are plotted. Complete plots are shown in Fig. 7 of Supplementary Information. Eight parameters representing major environmental factors for plant growth (temperature, humidity, and sunlight) in an area measured at a daily 1-km grid resolution from December 2010 to December 2011 were obtained from the Agro-Meteorological Grid Square Data System, NARO (<https://amu.rd.naro.go.jp/>)⁵⁵: daily mean air temperature, daily maximum air temperature, daily minimum air temperature, daily precipitation (reanalysis), mean relative humidity, global solar radiation, downward long-wave radiation, and sunshine duration. The correlation analysis was performed using the `lm()` function in R⁵⁴.

Productivity analysis and correlation analysis of species diversity and meteorological parameters of synecoculture field B (Fig. 4)

78 kinds of vegetable and fruit products were harvested from field B and sold as delivery boxes from January 2011 to February 2014 at a price rate of 315 JPY per 100 g, which is approximately equivalent to the rate for certified organic products (about 1.5 times higher than the price of conventional farm products) in the same region (Supplementary Data 2). From June 2010 to May 2014, other edible plant products, seeds and seedlings were also occasionally harvested and sold on-site, including as ingredients for a local restaurant; the data are summarized for each month (Supplementary Data 3). The principal cost was comparable to that of the conventional methods and comprised the cost of seeds and seedlings (Supplementary Data 4).

Yearly average data of productivity (gross sales in JPY) and material costs (seeds and seedlings, fertilizers and other amendments, materials such as plastic mulch, and machinery such as a tractor) of open-field conventional market gardening during 2010–2014 were obtained from the online database provided by the Ministry of Agriculture, Forestry and Fisheries in Japan⁵⁶. These datasets were converted into amounts per 1000 sq.m. The probability density functions shown in Fig. 4a were numerically estimated using the `density()` function in R⁵⁴.

To compare the yearly summed productivity of the conventional methods and with the daily recorded productivity of synecoculture, the scale of the *x*-axis of Fig. 4a is each unit sale multiplied by the number of harvest events per year. The conventional data consists of the yearly mean gross sales $X_c = \sum_{i=1}^n c_i$ that comprise those of *n* harvest events $\{c_i\}$, which are not

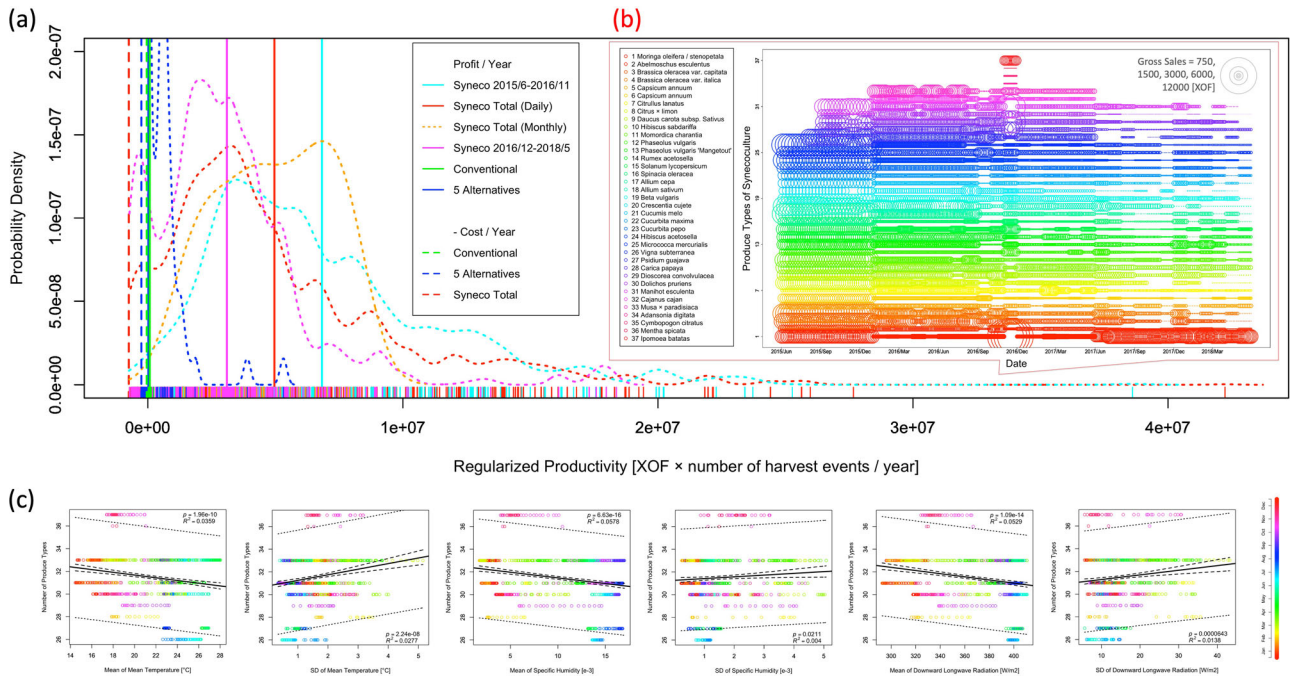


Fig. 5 | Productivity of synecoculture experiment in the tropical semi-arid zone (field C). The three-year production experiment in Mahadaga, Burkina Faso shows a power-law distribution of product sales with (b in the red rectangle) asynchronous harvests of 37 kinds of crop. The *x*-axis of a represents sales of each product for synecoculture and for five alternative farming methods that were simultaneously tested on 500 sq.m (regularized productivity is daily and species-wise productivity in terms of West African CFA franc (XOF) multiplied by the number of harvest events per year for synecoculture and five alternative farming methods or yearly reported profit for the conventional methods), both with an offset of total costs in order to compare the yearly mean profits (vertical solid lines) and costs (vertical dashed lines) summed as positive and negative values, respectively (see Methods). The dotted lines represent the estimated probability distributions for each production category on the *y*-axis based on the data shown by the rug plots along the *x*-axis. The total productivity of synecoculture (red line and distribution) is shown on a monthly

aggregated scale (orange distribution) and in the two periods before (cyan line and distribution) and after (magenta line and distribution) November 2016, which was the turning point of market accessibility (see Methods). In b left, the 37 academic names of total synecoculture products are shown as a list with a color gradient, and the associated numbers define the value of the *y*-axis in b right, in which the sales of each product according to date on the *x*-axis is represented as the diameter of the circle with the same color gradient as the list. The correlational analysis in c shows significant positive correlations between the number of produce types from synecoculture and meteorological variances for each 14-day interval. There are also significant negative correlations with the means of the meteorological parameters. Harvested crop diversity versus mean or variance of three meteorological parameters is plotted as circles following the color gradient of the year's date. Black solid line: linear regression with less than 5% significance; dashed line: linear regression with 95% confidence; dotted line: linear regression with prediction intervals.

explicitly shown in the dataset. *n* is usually small (a few times per year for each crop), and $\{c_i\}$ follows a normal distribution because it is based on a large sum of simultaneous harvests of monoculture crops; therefore, X_c is a good representative value of $\{c_i\}$. One can compare X_c with the yearly summed gross sales of synecoculture $X_s = \sum_{i=1}^m s_i$ based on the record of *m* harvest events $\{s_i\}$ in daily and species-wise resolution, which is shown as vertical solid lines and rug plots in Fig. 4a. In synecoculture, *m* is large (yearly average, *m* = 285 for the field B and *m* = 3619 for the field C), and $\{s_i\}$ follow a power-law distribution (also plotted in Fig. 10 of Supplementary Information). Therefore, $\{s_i\}$ contains a large deviation from X_s . In order to plot $\{s_i\}$ on a compatible scale with X_c and X_s , we need to define the regularized productivity $r_i = m \cdot s_i$ (daily and species-wise productivity s_i multiplied by the number of harvest events *m* on a yearly scale), because in that way the mean value of $\{r_i\}$ coincides with X_s , i.e., $X_s = \sum_{i=1}^m s_i = \sum_{i=1}^m m \cdot s_i / m = \frac{1}{m} \sum_{i=1}^m r_i$, regardless of the frequency of harvest events. The same scale applies to the yearly costs that are expressed as a negative offset to gross sales, which is depicted with the vertical dashed lines in Fig. 4a.

The correlation between the number of produce types (product diversity measured by the number of different species) sold as delivery box and the mean and standard deviation of eight major meteorological parameters⁵⁵ (same as in the field A experiment) for each 30-day interval was analyzed. Typical results are shown in Fig. 4c; complete plots are shown in Fig. 8 of Supplementary Information.

Productivity analysis and correlation analysis between species diversity and meteorological parameters of synecoculture field C (Fig. 5)

Products from 37 plant species in field C were harvested and sold at a local market from June 2015 to May 2018^{53,57,58}. The price rate was set to those of organic products (about two times higher than conventional products) from June 2015 to May 2017, and to the prices of conventional products from June 2017 to May 2018, because of deterioration of local security situation and consequent loss of customers.

Five alternative methods that aim for sustainable farming were also tested alongside the synecoculture production during the same period, namely 1: a system of rice intensification and trees, 2: conservation agriculture, 3: permaculture, 4: bio-intensive market gardening, and 5: traditional market gardening. We obtained the gross sales of synecoculture sales at a daily resolution (Supplementary Data 5) and those of the five alternative methods in terms of the monthly aggregated sum (Supplementary Data 6), together with the monthly installation, materials and working costs (Supplementary Data 7).

Conventional market gardening data based on the estimation of ten crops in Burkina Faso was obtained from a Food and Agriculture Organization of the United Nations (FAO) document⁵⁹ on standards of gross sales and costs, which included only installation and water costs and excluded other operation costs such as seeds and seedlings, fertilizer and phytosanitary products, and materials and working costs.

Datasets of gross sales and costs of the five alternative and conventional methods were converted into amounts per 500 sq.m. The probability density functions in Fig. 5a were numerically estimated using the density() function in R⁵⁴. The x-axis in Fig. 5a conforms to that of Fig. 4a.

In regard to Fig. 5c, satellite meteorological data corresponding to the field C at a daily 19.2-km grid resolution was obtained from (<http://clim-engine.appspot.com/>)⁶⁰. From which, 19 major parameters related to plant growth were taken from the Climate Forecast System (CFS) Reanalysis dataset of the National Centers for Environmental Prediction (NCEP): maximum temperature, mean temperature, minimum temperature, potential evaporation, precipitation, specific humidity, maximum specific humidity, minimum specific humidity, 5-cm soil moisture, 25-cm soil moisture, 70-cm soil moisture, 150-cm soil moisture, net radiation, downward shortwave radiation, upward shortwave radiation, downward longwave radiation, upward longwave radiation, latent heat flux, and sensible heat flux.

The correlation between the number of produce types (product diversity measured by the number of different species) and the means and standard deviations of the meteorological parameters for each 14-day interval (a substantial period of growth of crops in the field) were analyzed. Typical results are illustrated in Fig. 5c; the complete plots are shown in Fig. 9 of Supplementary Information.

Estimation of harvest biomass from product sales

Although the land equivalent ratio (LER)⁵¹ is used to evaluate polyculture productivity, it is not suitable for evaluating highly diverse mixed polycultures for two reasons:

1. For any probability distribution with the mean ν and standard deviation σ , the effect of fluctuations expressed as a ratio $\frac{\nu \pm \sigma}{\nu \pm \sigma}$ is not symmetric with respect to the standard ratio $\frac{\nu \pm 0}{\nu \pm 0} = 1$, which results in the LER having a positive bias; e.g., $\left(\frac{\nu + \sigma}{\nu + \sigma} + \frac{\nu - \sigma}{\nu - \sigma} + \frac{\nu + \sigma}{\nu - \sigma} + \frac{\nu - \sigma}{\nu + \sigma}\right) / 4 = \frac{\nu^2}{\nu^2 - \sigma^2} > 1$. Therefore, even if the monoculture and polyculture productivities are equal, the effect of fluctuation in LER gives a positive bias to polyculture.
2. Actual monoculture productivity data is a weighted sum of many monoculture crops^{56,59}, which is equivalent to a polyculture based on a mosaic of different monoculture surfaces. Therefore, the proportion of each crop surface within a given social-ecological context affects the overall productivity, which is not considered to be a realistic constraint in LER.

To overcome this pitfall, we defined the relative biomass ratio (BR) that represents the community-based land equivalent ratio as follows:

$$BR := \frac{\sum_{i=1}^k X_i}{\sum_{j=1}^l Y_j}$$

Where X_i is the mixed polyculture yield ($k > 1$ crops are mixed together on the same surface) of the i th crop, and Y_j is the mosaic polyculture yield (a combination of separate monocultures with $l > 1$ different crops on the same surface area) of the j th crop. Note that BR coincides with $LER := \sum_{i=1}^k \frac{X_i}{U'}$ in the IMPEO of one or more crops with the same physiological growth curve U' .

In the case that k crops for P_i are included in the l crops of Q_j , which is the case for field B, it is possible to calculate the BR of the mixed polyculture products using the sales data weighted with the per-price weight of each crop:

$$BR := \frac{\sum_{i=1}^k P_i \cdot V_i}{\sum_{j=1}^l Q_j \cdot W_j}$$

Where P_i and Q_j are the productivity measured by the sale price, V_i and W_j are product biomass per unit price for each crop ($X_i = P_i \cdot V_i$ and $Y_j = Q_j \cdot W_j$). In this study, the price rate R of synecoculture products are

set as $R := \frac{W_i}{V_i} \cong 1.5$ in field B. For field C, $R \cong 2.0$ and $R \cong 1.0$ for the first two years and the third year, respectively.

In sufficiently diverse sets of crops, the average product biomass per price defined as $V := \frac{\sum_{i=1}^k P_i \cdot V_i}{\sum_{i=1}^k P_i}$ and $W := \frac{\sum_{j=1}^l Q_j \cdot W_j}{\sum_{j=1}^l Q_j}$ converge to finite values, and their ratio converges to R , such that $\frac{W}{V} \approx R$. Using these relationships, the estimation of BR is obtained as follows:

$$BR \approx \frac{V \cdot \sum_{i=1}^k P_i}{W \cdot \sum_{j=1}^l Q_j} = \frac{\sum_{i=1}^k P_i / R}{\sum_{j=1}^l Q_j}$$

If k crops for P_i are not totally included in the l crops of Q_j , which is the case of field C, we considered the possible variable range of conventional productivity based on the median and 25th and 75th percentiles of productivity in l crops (see also Fig. 11 b2 of Supplementary Information).

This estimated biomass does not include the biomass of the established ecosystem permanently present in the synecoculture field, such as trees and seedlings, naturally occurring non-edible plants, fallen leaves, stems after harvest, and highly developed root systems that are sources of soil organic matter.

Power-law fitting of surface distribution and harvest sales in Fig. 10 of Supplementary Information

The probability density (y -axis) of the following variables (x -axis) was estimated using the density() function in R and linearly fitted with a Pareto distribution $Y = \frac{ab^x}{x^{a+1}}$ on a double-logarithmic scale by using the lm() function in R⁵⁴.

Field A: Species-wise surface percentage data for 80 2-sq.m sections in the Oiso farm (Supplementary Data 1). Surface data above 5% and the estimated probability density were used for the fitting.

Field B: Crop-wise daily sales data of the delivery box from the Ise farm (Supplementary Data 2). Sales data above 1000 JPY and the estimated probability density above 1.0e-7 were used for the fitting.

Field C: Crop-wise daily sales data of the Mahadaga farm (Supplementary Data 5). Sales data above 1000 XOF and the estimated probability density above 1.0e-7 were used for the fitting.

Data availability

Data is provided within the supplementary data file.

Received: 22 December 2023; Accepted: 15 March 2024;

Published online: 10 May 2024

References

1. Barnosky, A. D. et al. Approaching a state shift in Earth's biosphere. *Nature* **486**, 52–58 (2012).
2. Ripple, W. J. et al. World Scientists' warning to humanity: a second notice. *BioScience* **67**, 1026–1028 (2017).
3. Díaz, S. et al. Pervasive human-driven decline of life on Earth points to the need for transformative change. *Science* **366**, eaax3100 (2019).
4. Intergovernmental Science-Policy Platform on Biodiversity and Ecosystem Services (IPBES). *Global assessment report on biodiversity and ecosystem services of the Intergovernmental Science-Policy Platform on Biodiversity and Ecosystem Services*. (IPBES secretariat, Bonn, Germany, 2019).
5. McDowell, N. G. et al. Pervasive shifts in forest dynamics in a changing world. *Science* **368**, eaaz9463 (2020).
6. Ceballos, G., Ehrlich, P. R. & Raven, P. H. Vertebrates on the brink as indicators of biological annihilation and the sixth mass extinction. *Proc. Natl. Acad. Sci. USA* **117**, 13596–13602 (2020).
7. Sánchez-Bayo, F. & Wyckhuys, K. A. G. Worldwide decline of the entomofauna: a review of its drivers. *Biol. Conserv.* **232**, 8–27 (2019).

8. Diaz, R. J. & Rosenberg, R. Spreading dead zones and consequences for marine ecosystems. *Science* **321**, 926–929 (2008).
9. Smith, P. et al. In *Climate Change 2014: Mitigation of Climate Change. Contribution of Working Group III to the Fifth Assessment Report of the Intergovernmental Panel on Climate Change* (eds Edenhofer, O. et al.) 2014: Agriculture, Forestry and Other Land Use (AFOLU). (Cambridge University Press, 2014).
10. Steffen, W. et al. Planetary boundaries: Guiding human development on a changing planet. *Science* **347**, 1259855 (2015).
11. The Intergovernmental Panel on Climate Change (IPCC). *Global Warming of 1.5 °C Global Warming of 1.5 °C. An IPCC Special Report on the impacts of global warming of 1.5 °C above pre-industrial levels and related global greenhouse gas emission pathways, in the context of strengthening the global response to the threat of climate change, sustainable development, and efforts to eradicate poverty* (eds Masson-Delmotte, V. et al.) (2018).
12. Daszak, P. et al. *Workshop Report on Biodiversity and Pandemics of the Intergovernmental Platform on Biodiversity and Ecosystem Services* (IPBES secretariat, Bonn, Germany, 2020).
13. Costanza, R. et al. Twenty years of ecosystem services: How far have we come and how far do we still need to go? *Ecosyst. Serv.* **28**, 1–16 (2017).
14. Funabashi, M. Human augmentation of ecosystems: objectives for food production and science by 2045. *NPJ Sci. Food* **2**, 16 (2018).
15. Erb, K. H. et al. Exploring the biophysical option space for feeding the world without deforestation. *Nat. Commun.* **7**, 11382 (2016).
16. Bastin, J. F. et al. The global tree restoration potential. *Science* **365**, 76–79 (2019).
17. Sattari, S. Z., Bouwman, A. F., Rodríguez, R. M., Beusen, A. H. W. & van Ittersum, M. K. Negative global phosphorus budgets challenge sustainable intensification of grasslands. *Nat. Commun.* **7**, 10696 (2016).
18. Machmuller, M. B. et al. Emerging land use practices rapidly increase soil organic matter. *Nat. Commun.* **6**, 6995 (2015).
19. Veldman, J. W. et al. Comment on “The global tree restoration potential. *Science* **366**, eaay7976 (2019).
20. Lesiv, M. et al. Estimating the global distribution of field size using crowdsourcing. *Glob. Chang. Biol.* **25**, 174–186 (2019).
21. Ending hunger. science must stop neglecting smallholder farmers. *Nature* **586**, 336 (2020).
22. Altieri, M. A. Agroecology: the science of natural resource management for poor farmers in marginal environments. *Agr. Ecosyst. Environ.* **93**, 1–24 (2002).
23. Tokoro, M. Open Systems Science: A Challenge to Open Systems Problems. In *First Complex Systems Digital Campus World E-Conference 2015* (eds Bourguine, P., Collet, P. & Parrend, P.) 213–221 (Springer International Publishing, Switzerland, 2017).
24. Funabashi, M. et al. Foundation of CS-DC e-laboratory: open systems exploration for ecosystems leveraging. In *first complex systems digital campus World E-Conference 2015* (eds Bourguine, P., Collet, P. & Parrend, P.) 351–374 (Springer International Publishing, Switzerland, 2017).
25. Schork, N. J. Personalized medicine: Time for one-person trials. *Nature* **520**, 609–611 (2015).
26. Planetary Health Alliance. <https://www.planetaryhealthalliance.org/>.
27. Tilman, D. Diversity and productivity in a long-term grassland experiment. *Science* **294**, 843–845 (2001).
28. Scanlon, T. M., Caylor, K. K., Levin, S. A. & Rodriguez-Iturbe, I. Positive feedbacks promote power-law clustering of Kalahari vegetation. *Nature* **449**, 209–212 (2007).
29. Kéfi, S. et al. Spatial vegetation patterns and imminent desertification in Mediterranean arid ecosystems. *Nature* **449**, 213–217 (2007).
30. Funabashi, M. Synecological farming: theoretical foundation on biodiversity responses of plant communities. *Plant Biotechnol.* **32**, 1–22 (2016).
31. Funabashi, M. Augmentation of plant genetic diversity in Synecoculture: theory and practice in temperate and tropical zones. In *Genetic Diversity in Horticultural Plants* (ed. Nandwani, D.) 3–46 (Springer International Publishing, Switzerland, 2019).
32. Smith, J., Yeluripati, J., Smith, P. & Nayak, D. R. Potential yield challenges to scale-up of zero budget natural farming. *Nat. Sustain.* **3**, 247–252 (2020).
33. Lange, M. et al. Plant diversity increases soil microbial activity and soil carbon storage. *Nat. Commun.* **6**, 6707 (2015).
34. Funabashi, M. Synecological farming for mainstreaming biodiversity in smallholding farms and foods: implication for agriculture in India. *Indian J. Plant Genet. Resour.* **30**, 99–114 (2017).
35. Kéfi, S. et al. Early warning signals of ecological transitions: methods for spatial patterns. *PLoS ONE* **9**, e92097 (2014).
36. IIED & UNEP-WCMC. *Mainstreaming biodiversity and development: guidance from African experience 2012–17* (IIED, London 2017).
37. Rippke, U. et al. Timescales of transformational climate change adaptation in sub-Saharan African agriculture. *Nat. Clim. Chang.* **6**, 605–609 (2016).
38. Pecl, G. T. et al. Biodiversity redistribution under climate change: Impacts on ecosystems and human well-being. *Science* **355**, eaai9214 (2017).
39. Springmann, M. et al. Options for keeping the food system within environmental limits. *Nature* **562**, 519–525 (2018).
40. Berdugo, M., Kéfi, S., Soliveres, S. & Maestre, F. T. Plant spatial patterns identify alternative ecosystem multifunctionality states in global drylands. *Nat. Ecol. Evol.* **1**, 0003 (2017).
41. The Great Green Wall. <https://www.greatgreenwall.org/>.
42. Tilman, D. et al. Future threats to biodiversity and pathways to their prevention. *Nature* **546**, 73–81 (2017).
43. de Bruyn, J. et al. Food composition tables in resource-poor settings: exploring current limitations and opportunities, with a focus on animal-source foods in sub-Saharan Africa. *Br. J. Nutr.* **116**, 1709–1719 (2016).
44. Tchilalo, P., Tindano, A., & Funabashi, M. (eds.) *Actes du 6e Forum Africain sur la Synécoculture/Proceedings of the 6th African Forum on Synecoculture (French-English Version)*. Research and Education material of UniTwin UNESCO Complex Systems Digital Campus, e-laboratory: Human Augmentation of Ecosystems, No. 2 (2022).
45. Alexandratos, N. & Bruinsma, J. *World agriculture towards 2030/2050: the 2012 revision. ESA Working paper No. 12-03* (Rome, FAO 2012).
46. Stephenson, P. J. et al. Unblocking the flow of biodiversity data for decision-making in Africa. *Biol. Conserv.* **213**, 335–340 (2017).
47. Frelat, R. et al. Drivers of household food availability in sub-Saharan Africa based on big data from small farms. *Proc. Natl. Acad. Sci. USA* **113**, 458–463 (2015).
48. Jaenicke, H., Ganry, J., Hoeschle-Zeledon, I. & Kahane, R. (eds.) *International symposium on underutilized plants for food security, nutrition, income and sustainable development*. (Arusha, Tanzania, 2009).
49. Lowder, S. K., Skoet, J. & Raney, T. The number, size, and distribution of farms, smallholder farms, and family farms worldwide. *World Dev.* **87**, 16–29 (2016).
50. Herrero, M. et al. Farming and the geography of nutrient production for human use: a transdisciplinary analysis. *Lancet Planet. Health* **1**, e33–e42 (2017).
51. Mead, R. & Willey, R. W. The concept of a ‘land equivalent ratio’ and advantages in yields from intercropping. *Exp. Agric.* **16**, 217–228 (1980).
52. Funabashi, M. (editor) *Synecoculture Manual 2016 Version (English Version)* Research and Education material of UniTwin UNESCO Complex Systems Digital Campus, e-laboratory: Open Systems Exploration for Ecosystems Leveraging, No. 2. (2016).
53. Tindano, A. & Funabashi, M. (eds) *Proceedings of the 1st African Forum on Synecoculture (English Version)*. Research and Education

- material of UniTwin UNESCO Complex Systems Digital Campus, e-laboratory: Open Systems Exploration for Ecosystems Leveraging, No. 5. (2017).
54. R Core Team. R: A language and environment for statistical computing (R version 3.6.0.). (R Foundation for Statistical Computing, Vienna, Austria, 2019). <https://www.r-project.org/>.
 55. Ohno, H., Sasaki, K., Ohara, G. & Nakazono, K. Development of grid square air temperature and precipitation data compiled from observed, forecasted, and climatic normal data. *Clim. Biosph.* **16**, 71–79 (in Japanese with English title) (2016).
 56. M.A.F.F e-stat. Ministry of Agriculture, Forestry and Fisheries of Japan. <http://www.e-stat.go.jp/SG1/estat/List.do?lid=000001089733>.
 57. Tindano, A. & Funabashi, M. (eds) *Proceedings of the 2nd African Forum on Synecoculture (English Version)*. Research and Education material of UniTwin UNESCO Complex Systems Digital Campus, e-laboratory: Open Systems Exploration for Ecosystems Leveraging, No.7. (2018).
 58. Tindano, A. & Funabashi, M. (eds) *Proceedings of the 3rd African Forum on Synecoculture (English Version)*. Research and Education material of UniTwin UNESCO Complex Systems Digital Campus, e-laboratory: Open Systems Exploration for Ecosystems Leveraging, No. 10. (2018).
 59. FAO EASYPol. Analyse de la filière maraichage au Burkina Faso. Ressources complémentaires, Module EASYPol 107. http://www.fao.org/docs/up/easypol/887/analyse-filiere-maraichage_107fr.pdf (2017).
 60. Huntington, J. L. et al. Climate Engine: cloud computing and visualization of climate and remote sensing data for advanced natural resource monitoring and process understanding. *Bull. Amer. Meteor. Soc.* **98**, 2397–2410 (2017).
- Développement Rural Autogéré (AFIDRA) and Centre Africain de Recherche et de Formation en Synécoculture (CARFS) under the direction of André Tindano. Fig. 6 of Supplementary Information was drawn by courtesy of Kei Fukuda.

Author contributions

M.F. performed data analysis, wrote the manuscript, and prepared the figures.

Competing interests

The author declares no competing interests.

Additional information

Supplementary information The online version contains supplementary material available at <https://doi.org/10.1038/s44264-024-00014-4>.

Correspondence and requests for materials should be addressed to Masatoshi Funabashi.

Reprints and permissions information is available at <http://www.nature.com/reprints>

Publisher's note Springer Nature remains neutral with regard to jurisdictional claims in published maps and institutional affiliations.

Open Access This article is licensed under a Creative Commons Attribution 4.0 International License, which permits use, sharing, adaptation, distribution and reproduction in any medium or format, as long as you give appropriate credit to the original author(s) and the source, provide a link to the Creative Commons licence, and indicate if changes were made. The images or other third party material in this article are included in the article's Creative Commons licence, unless indicated otherwise in a credit line to the material. If material is not included in the article's Creative Commons licence and your intended use is not permitted by statutory regulation or exceeds the permitted use, you will need to obtain permission directly from the copyright holder. To view a copy of this licence, visit <http://creativecommons.org/licenses/by/4.0/>.

© The Author(s) 2024

Acknowledgements

This study was funded by Sony CSL. The field experiment in Oiso, Japan was conducted by M.F. and supported by Kiyomi Kondo-Nishikata, Akira Tamaki, and research assistants of Sony CSL: Hidemori Yazaki, Kousaku Ohta, Tatsuya Kawaoka, Kazuhiro Takimoto, and Shuntaro Aotake. The synecoculture production experiment in Ise, Japan was conducted by Sakura Shizenjyuku, Inc. under the direction of Takashi Otsuka, and in Mahadaga, Burkina Faso by Agence de Formation et d'Ingénierie du